

# FUZZY INFERENCE ENHANCED INFORMATION RECOVERY FROM DIGITAL PIV USING CROSS-CORRELATION COMBINED WITH PARTICLE TRACKING

Mark P. Wernet  
National Aeronautics and Space Administration  
Lewis Research Center  
Cleveland, Ohio 44135

## ABSTRACT

Particle Image Velocimetry provides a means of measuring the instantaneous 2-component velocity field across a planar region of a seeded flowfield. In this work only two camera, single exposure images are considered where both cameras have the same view of the illumination plane. Two competing techniques which yield unambiguous velocity vector direction information have been widely used for reducing the single exposure, multiple image data: cross-correlation and particle tracking. Correlation techniques yield averaged velocity estimates over subregions of the flow, whereas particle tracking techniques give individual particle velocity estimates. The correlation technique requires identification of the correlation peak on the correlation plane corresponding to the average displacement of particles across the subregion. Noise on the images and particle dropout contribute to spurious peaks on the correlation plane, leading to misidentification of the true correlation peak. The subsequent velocity vector maps contain spurious vectors where the displacement peaks have been improperly identified. Typically these spurious vectors are replaced by a weighted average of the neighboring vectors, thereby decreasing the independence of the measurements. In this work fuzzy logic techniques are used to determine the true correlation displacement peak even when it is not the maximum peak on the correlation plane, hence maximizing the information recovery from the correlation operation, maintaining the number of independent measurements and minimizing the number of spurious velocity vectors. Correlation peaks are correctly identified in both high and low seed density cases. The correlation velocity vector map can then be used as a guide for the particle tracking operation. Again fuzzy logic techniques are used, this time to identify the correct particle image pairings between exposures to determine particle displacements, and thus velocity. The advantage of this technique is the improved spatial resolution which is available from the particle tracking operation. Particle tracking alone may not be possible in the high seed density images typically required for achieving good results from the correlation technique. This two staged approach offers a velocimetric technique capable of measuring particle velocities with high spatial resolution over a broad range of seeding densities.

## INTRODUCTION

Digital Particle Image Velocimetry (DPIV) provides a means of measuring the instantaneous 2-component velocity field across a planar region of a seeded flowfield. A pulsed laser light sheet is used to illuminate the seed particles entrained in the flowfield. One or more CCD cameras can be used to record the instantaneous particle positions. The all

digital approach to PIV has gained more widespread interest with increased pixel count CCD cameras. The digital recording system eliminates the most time consuming and laborious tasks in conventional photographic PIV: film developing and mechanical interrogation of the developed film. Although photographic film offers higher spatial resolution than today's CCD technology, higher pixel count cameras are certain to become available driven by such technologies as High Definition Television (HDTV). HDTV technology may lead to a secondary added benefit of reduced image storage requirements via improved image compression techniques.

When two CCD cameras are used to record single exposure particle image records, two competing data reduction techniques are available for reducing the data: cross-correlation on small subregions of the two images, or tracking the images of particles recorded on the two independent image frames. The second camera replaces the complex galvanometer/mirror system typically used to record dc-offset double exposure, single image frames used in auto-correlation analysis systems to achieve velocity vector direction information. Cross-correlation of two single exposure image frames eliminates the self-correlation peak on the output plane, provides unambiguous determination of the velocity vector direction, and maximizes the dynamic range of the measured velocity magnitudes by allowing particle image overlap between the two exposures. Previous work on cross-correlation or particle tracking for multi-frame, single exposure images has been restricted to low velocity flows ( $<1$  m/s) where NTSC/PAL video systems have determined the limiting framing rate (Westerweel & Nieuwstadt, 1990, Wernet & Plin, 1991, Willert & Gharib, 1991, Kemmerich & Rath, 1994). By adjusting the exposure period in standard video systems to occur at the very end of a video field and right at the start of the next video field a pair of single exposure image fields can be obtained with an effective high framing rate so that high velocity flows can be measured via particle tracking (Wernet, 1991). Most other all digital high speed flow measurements have been made via auto-correlation analysis of multi-exposure, single frame image data (Westerweel et. al., 1994). Particle tracking techniques for air flows have been limited to low seed density regimes in order to avoid confusion in correctly identifying the particle pairings (Funes-Gallanzi & Bryanston-Cross, 1993). Particle tracking by itself is typically not capable of successfully tracking particles at the high seed particle densities normally used for auto- or cross-correlation analysis. Conversely, correlation techniques must use large subregion sizes, with a concomitant reduction in spatial resolution, in order to perform adequately in the low seed density regimes where particle tracking techniques are normally applied. The possibility of combining the high precision of the auto- or cross-correlated velocity vector maps with the high spatial resolution offered by particle tracking techniques has been proposed, but not yet implemented (Keane & Adrian, 1993). The combined technique would provide high spatial resolution velocity measurements across a broad range of seed particle concentrations.

The correlation processed PIV images always result in at least a few erroneous velocity vectors. The erroneous detections can be divided into two classes: class I where there is insufficient information to estimate the average displacement across the subregion; and class II where there is a noise peak of greater amplitude than the true correlation peak (Raffel, et. al 1992). The erroneous vectors resulting from class I type errors can only be corrected by interpolation or extrapolation of the surrounding data in a post-processing step. Many techniques have been proposed for correcting these class I type errors (Raffel et. al., 1992,

Meinhart et. al., 1992, Host-Madsen & McCluskey, 1994). Before resorting to the class I type solution, the correlation plane must be carefully examined to ensure that the true displacement information cannot be recovered. The highest peak may not be the true displacement; however, the correct displacement peak must exist in the correlation plane provided enough particle image pairs were recorded within the subregion. Even the dreaded two particles in the interrogation region case still results in a correct displacement peak, although it may be confused with the random particle orientation correlation. The class II errors can be corrected by examining the other secondary peaks on the correlation plane and applying an appropriate validation algorithm (Meinhart et. al., 1992, Raffel, et. al. 1992)

In this work an all electronic, high speed cross-correlation/particle tracking technique is demonstrated which uses a fuzzy logic inference engine to maximize the information recovery from the correlation plane. A high resolution, two camera recording system utilizing a polarization beamsplitting cube for common viewing of the illumination plane provides two single exposure frames of the flow field, with no restriction on the interframe exposure time interval. A pair of pulsed Nd:YAG lasers is used to illuminate the seeded supersonic flow from a convergent nozzle operated in an underexpanded condition. The acquired image pairs are cross-correlated to obtain a regular grid velocity vector map. Erroneous velocity vectors are corrected by using a fuzzy inference engine to examine the secondary and lower amplitude peaks in the correlation plane (class II errors) and replace the erroneous vector with the correct velocity vector based on information from the surrounding velocity vectors. In this manner the correlation plane peak detection is treated as a pseudo particle tracking process where all of the peaks in the correlation plane are treated as candidate displacement peaks. Flow continuity rules govern the fuzzy inference engine to correctly identify the true correlation displacement peak. In the last step, the corrected velocity vector map is used as a guide for a fuzzy inference particle tracking analysis of the recorded images. The particle tracking technique is successful even in the high seed density required for the cross-correlation analysis. A velocity vector map with more than 3 times the spatial resolution of that obtained via cross-correlation is thus obtained. The automated data validation routine requires no operator information, and is shown to perform well even in the presence of a large velocity gradient caused by a Mach disk in the underexpanded flow field.

## FUZZY INFERENCE FOR DETECTING VELOCITIES

### Fuzzy Logic Particle Tracking

The use of fuzzy inference to track particles from a pair of digitally recorded, single exposure image frames has previously been described by Wernet, 1992. Briefly, the technique is simply the application of the rules of flow continuity. Velocity vectors located close to each other must be of similar magnitude and point in roughly the same direction. In the application to particle tracking, all possible second exposure particles located within a nominal 10 pixel region about a first exposure particle are deemed candidate velocity vectors and stored in an array. Some of the independent initial exposure particles will compete with each other for the same second exposure particle; therefore they must be close enough to follow the continuity rules above. All pairs of vectors from this interacting set of initial particles are then compared on a pair-wise basis. The pair of vectors possessing the most

similar qualities (magnitude, flow angle, particle size and shape) are deemed to be the correct particle displacement pair and assigned a confidence weighting by the fuzzy inference engine based on the degree of similarity. The process is repeated for all interacting vectors. The vectors for each initial particle with the highest weight are the correct displacements. The fuzzy inference engine runs completely in software and processes an image pair in a matter of seconds. The fuzzy weights in the rule base and membership functions are generic and applicable to a wide class of flow fields.

### Fuzzy Logic Correlation Peak Optimization

The particle tracking fuzzy inference engine has been applied in this work to the detection of the correct cross-correlation plane displacement peak. Ideally, when the image data are of high quality and high seed density the highest amplitude peak on the correlation plane represents the average displacement of particles across the subregion being processed. However, particle out-of-plane motion, velocity gradients, image noise, or low particle concentration are all contributing sources for a noise peak to be misidentified as the average particle displacement across the subregion. In these cases the peak corresponding to the average motion of the particles across the subregion between exposures is not the highest amplitude peak, and possibly not even the second highest amplitude peak on the correlation plane. Traditionally, these spuriously detected velocity vectors are removed from the velocity vector maps via a postprocessing filtering operation. Any spurious vectors are replaced by the weighted average of the surrounding subregion velocity vectors, which reduces the independence of the velocity estimates.

The cross-correlations are computed on equal sized subregions from each of the single exposure CCD images. The subregions are zero padded to twice their initial dimensions to avoid wrap around error. The zero padded arrays are Fast Fourier Transformed, complex multiplied together, and then an inverse Fast Fourier Transform is applied. The resultant array is multiplied by its complex conjugate to obtain the intensity field on the correlation plane. The cross-correlation plane is scanned for peaks using an initial threshold level of 25% of the highest amplitude pixel in the correlation plane. If less than 5 peaks are detected the threshold level is reduced by 25% four more times or until at least 5 peaks are located. When peaks are detected the centroids are computed via a 3×3 weighted average about the highest amplitude pixel.

After all subregions in the image have been processed, the fuzzy inference operation is applied. The five highest amplitude peaks detected on the correlation plane are treated as candidate velocity vectors for this grid point as in the fuzzy PTV technique described above. Again we seek to have flow continuity as in the particle tracking methodology. The stored correlation peaks from each subregion are compared on a pairwise basis to the surrounding 4 subregion results. The displacement peaks resulting in velocity vectors with the most similar qualities are given the highest confidence weighting. The highest confidence weighting velocity vector for each processed subregion is taken as the correct correlation displacement peak. Hence, the fuzzy inference technique is very similar to the weighted average replacement technique, except that the surrounding velocity vectors are used to identify the correct displacement peak instead of merely replacing the spurious vector.

## COMBINED FUZZY CORRELATION PEAK DETECTION WITH PARTICLE TRACKING

The availability of a high quality velocity vector map obtained from the cross-correlation operation offers the opportunity to perform particle tracking on length scales smaller than the correlation subregion size. Instead of using the nearest neighbor and flow continuity approach to track particles, the correlation velocity vector map can be used as a guide for the particle tracking. Using the same two single exposure image frames from the computed cross-correlation step, the first exposure image is scanned for particle centroids. All second exposure particles located within a user specified search region around each first exposure particle are detected and stored. Next, the fuzzy inference engine is employed to determine which detected particle pairings are correct. The first exposure particles and their associated list of candidate second exposure particles are now individually examined. The four nearest neighboring velocity vectors from the cross-correlation vector map to the initial particle location are found and used to compute a spatially weighted mean velocity vector, called a "benchmark vector". The benchmark vector is then used in a pairwise fuzzy comparison with all of the candidate vectors in the list for this initial particle. The candidate vector most similar to the benchmark vector, is assigned the highest confidence weighting. Benchmark vectors are computed for all remaining initial particle locations and used to identify the most probable velocity vector for each initial particle.

## EQUIPMENT

The single exposure particle image frames were obtained via a dual laser, dual camera data acquisition system as depicted in figure 1. Two frequency doubled Nd:YAG lasers were used to provide the 200 mJ/pulse light sheet illumination. A wavelength separation/beam combining unit was used to obtain orthogonally polarized, coaxial beams from the two lasers after frequency doubling. The nominal 6 mm diameter beam from the YAG lasers was shaped into a  $0.5 \times 50$  mm light sheet via -40 mm and 400 mm focal length cylindrical and spherical lenses, respectively.

A digital delay generator was used to control the relative timing between lasers A and B, where the first pulse came from laser A and the second pulse from laser B. The pulse generator was set for a repetition rate of 10 Hz. An initialization pulse from the delay generator was used to fire both YAG laser flashlamps simultaneously. A second pair of pulses were used to fire the Q-switches of the two lasers yielding a relative timing error of  $\pm 2$  nsec. The two lasers were first made to fire simultaneously by adjusting the relative time delay between the Q-switch pulses for both lasers and by verifying the pulsed light output times using a photodiode. The time delay between the two laser pulses was then obtained by increasing the time delay for firing the B laser Q-switch.

The recording system consisted of two Kodak Megaplug 1.4 cameras with  $1320 \times 1040 \times 8$  bit pixel resolution mounted in a common viewing arrangement via a polarization beamsplitting cube. The table containing the beam splitter/camera system was mounted on a translation stage which allowed positioning the focal plane of the detection system in the plane of the light sheet. The polarization separation between cameras is required since the Kodak cameras use mechanical shutters with a minimum response time of 12 msec. Hence,

for the supersonic velocities under study here, both camera shutters would be open simultaneously. The light scattered by particles in the light sheet passed through the polarizing beamsplitting cube before reaching the cameras. Camera A was only sensitive to the *s*-polarized light reflected 90° by the beamsplitter while camera B detected *p*-polarized light passing straight through the beamsplitter. Two EPIX framegrabber boards were used in a 80486/66 PC to acquire the image data from the Kodak cameras via an analog interface. Camera A viewed a mirror image of the view obtained by camera B due to the 90° reflection in the beamsplitter. The image was reversed using the framegrabber DSP chip for both display on a video monitor and before storing to disk. The cameras were equipped with 50 mm focal length lenses operating at *f*/5. The shutter times on the cameras were set at 100 ms to enable the capture of a single laser pulse.

The camera mounts were mechanically adjusted to achieve a near perfect registration of the image plane on both cameras. To eliminate any residual registration errors or optical distortions a reference grid was placed in the image plane and recorded by both cameras. The reference grid contained 0.5 mm black dots located on 2.54 mm centers, where a grid cell is defined as a set of 4 grid points outlining a square. A set of bilinear image warping coefficients was computed for each grid cell in each camera image so that both images were pixel registered across the entire image plane. Although the image distortions from the lens and/or beamsplitting cube may be non-linear, we assume that the distortions are linear within each grid cell. All subsequent data imagery were warped to the reference grid before processing the data to determine velocity information. Any optical distortions or magnification mismatch in the optical system between the cameras were eliminated via this procedure. Knowledge of the grid cell size in pixels also provided the image scale. For the configuration shown the image scale was 45 μm/pixel, corresponding to a 60 × 47 mm field of view.

The flowfield was generated by a convergent nozzle operated at underexpanded conditions. Under these conditions a Mach disk is generated in the flow field providing a sharp deceleration in velocity across the normal shock. The nozzle plenum chamber was fitted with coarse mesh followed by fine mesh screens for flattening out the velocity profile before the convergent section to the nozzle exit (diameter = 6.35 mm). The light sheet was directed vertically across the exit flow oriented with the 50 mm dimension along the flow direction. The flow was seeded in the nozzle plenum chamber with a TSI 6-jet atomizer filled with Rosco's Smoke Juice, which produced seed particles with a mean diameter of approximately 1 micron. All data acquisition and data processing was performed on a 80486/66 PC.

## RESULTS AND DISCUSSION

Particle imagery data were obtained from the supersonic flow generated from the convergent nozzle operated at a plenum pressure and temperature of 517 kPa (74 psia) and 294 K, respectively. Under these conditions the Mach disk is located approximately 1.5 diameters downstream from the nozzle exit (Adamson & Nicholls, 1959). The flow conditions upstream of the Mach disk assuming an isentropic expansion are  $M=3.25$

( $U=633$  m/s) and a density of  $0.35$  kg/m<sup>3</sup>. Downstream of the shock the Mach number drops to  $0.46$  ( $U=155$  m/s) and the density rises to  $1.4$  kg/m<sup>3</sup>. Two single exposure PIV images were acquired with a time delay between exposures of  $500$  nsec. Figure 2 shows a sample single exposure image acquired by the data acquisition system. The position of the Mach disk is indicated in the figure by the vertical white line. The number of seed particles upstream of the shock is markedly less than the observed concentration downstream of the shock, due to the large density change across the shock. Less than 1% of the particles in the image depolarize a sufficient amount of the scattered light to be detected by the orthogonal polarization sensitive camera. Hence, depolarization did not cause a problem in obtaining single exposure images of the particles.

The data processing operations occurred in two separate stages: cross-correlation; and particle tracking. Both operations used fuzzy inference techniques to maximize information recovery. The cross-correlation operation was performed by first warping the images to a Cartesian reference grid. Next,  $32 \times 32$  equal sized subregions from both images A and B were cross-correlated via FFTs. The subregions were spaced on 32 pixel centers so that no overlap between subregions occurred.

Figures 3(a) and 3(b) show the cross-correlation results with and without the fuzzy peak detection scheme. The vector magnitudes are color coded as shown in the color bar. Measured velocities in excess of  $600$  m/s are shown in pink while subsonic velocities are depicted in green and yellow. None of the bad vectors have been manually removed or filtered from either of the vector maps. In the fuzzy processing step there is a lower limit on the vector magnitude of  $0.9$  m/s ( $0.01$  pixels). Any vectors below this threshold were removed. Figure 3(b) contains 262 velocity vectors. In the central portion of the image in figure 3(b), where the particle concentration is high and the light sheet intensity is high, there are very few incorrectly identified correlation peaks. Most of the falsely identified peaks are in the periphery of the jet flow and light sheet. The fuzzy peak detection has correctly identified 26 class II erroneous vectors which otherwise would have been incorrectly identified in figure 3(b). A few of the vectors have been removed because their optimally identified correlation peaks resulted in a vector magnitude less than  $0.9$  m/s, leaving 229 velocity vectors in figure 3(a). A few class I type erroneous vectors remain in the image. The total processing time for the cross-correlation operation was 172 seconds. The time for the fuzzy correlation peak validation is approximately 2 seconds. The storage and processing requirements required to perform the fuzzy peak validation are minimal. The technique correctly replaced 11% of the vectors which were initially erroneously identified and did not increase the number of erroneous vectors in the image. No user input was required for the fuzzy peak detection operation.

The second step in the data processing was to perform the fuzzy particle tracking using the cross-correlation map in figure 3(a) as a guide for the particle tracking. The results of the fuzzy particle tracking operation are shown in figure 4, where 2369 vectors have been identified. Again a color map has been used to enhance the regions of high and low velocity. The vector magnitudes have been magnified to enhance their visibility, hence the crossed particle trajectories observed in the figure are an artifact of this scaling. The high data density melds the velocity vectors together; however, by adding a color map to the vector

magnitudes a pseudo contour plot is obtained. The total processing time for the fuzzy particle tracking operation was 38 seconds.

In figures 3(a) and 4 the underexpanded characteristics of the flow are evident. The flow is expanding outward as it exits the nozzle and then converges rapidly forming a barrel shape. The Mach disk is located at an axial position of 1.5 nozzle diameters, which agrees with our computed normal shock position. The very high data density obtained from the particle tracking gives a good overall picture of the jet structure. The supersonic core flow (pink vectors) is observed to decelerate very quickly across the shock (green, yellow and orange vectors). The flow accelerates again (pink/purple) and again decelerates across a second weaker shock (green/blue). A third acceleration/ deceleration region is also evident in the flow. The particle tracking result reveals much finer flow structure and higher dynamic range than the cross correlation vector maps.

Another comparison of the detected flow fields is obtained by plotting the axial velocity along the nozzle centerline, as shown in figure 5. The nozzle centerline is taken as the most centrally located row from the cross-correlation map. The nozzle location and Mach disk location are also depicted in figure 5. The cross-correlation result underpredicts the high velocity nozzle exit flow and also does not show the predicted velocity drop across the shock. The particle tracking result agrees with the high velocity prediction upstream of the shock and also depicts the large velocity drop across the shock. Each pixel is 45  $\mu\text{m}$ , therefore the particle tracking result shows that the particles in the flow decelerate within approximately 2 mm downstream of the shock. The scatter in the particle tracking velocity estimates can be attributed to particle lag effects and a small variation in the seed particle size.

After the first normal shock, the flow accelerates again to supersonic, and shocks down across a weaker normal shock. The particle tracking result shows this acceleration/deceleration having much higher peaks and valleys than the corresponding cross-correlation result. In general, the cross-correlation result appears as a low pass filtered version of the flow, which is expected from the inherent averaging over the subregions. The spatial resolution of the cross-correlation technique could be improved by increasing the seeding density and decreasing the subregion size; however, the low pass nature would still pervade the results and increasing the seed particle concentration is not always practical. The particle tracking technique, while not always providing a nice smooth picture of the flow field, is demonstrated here to offer superior spatial resolution over the cross-correlation technique. The  $32 \times 32$  pixel subregions used in the cross-correlation analysis yield a spatial resolution of 1.4 mm. The particle tracking technique has resolved ten times as many velocity vectors as the cross-correlation technique over the same measurement area. Hence, the particle tracking spatial resolution is on average more than a factor of 3 higher in the x- and y-dimensions. The two data processing techniques complement each other when used in concert. While the cross-correlation result is not required to perform the particle tracking in moderate seed density cases, it does result in a faster and higher success rate data reduction. For high seed particle concentrations, as shown here, the use of the cross-correlation map is required for high quality, low error rate particle tracking.

Another comparison plot of the two techniques is shown in figure 6 for a second data set. The flow conditions are identical to that shown in figure 5 above. In figure 6 the particle

tracking estimates are more tightly grouped downstream of the initial Mach disk. A few large diameter particles are observed as high velocity measurements just downstream from the Mach disk location, where the flow should have decelerated. Again the cross-correlation estimates show a low-pass filtered version of the flow. The velocity just upstream of the normal shock agrees with the particle tracking estimates. Downstream of the initial shock the cross-correlation estimate is lower than the expected velocity, which may be caused by an improper correlation peak identification at this location.

## CONCLUSIONS

The use of fuzzy inference techniques to maximize the information recovery from cross-correlation data has been demonstrated. The highest peak on the correlation plane does not always correspond to the average particle displacement across the correlation subregion. By using fuzzy processing techniques to examine the five largest peaks from each correlation subregion with the peaks from other subregions, continuity in the flow can be used to decipher the correct displacement peaks when amplitude alone is not sufficient to properly detect the velocity displacement. No significant performance penalty is incurred by performing this extra fuzzy peak detection step. Correctly identifying the correlation peaks maximizes the information recovery and also maximizes the independence of the measurements.

New processing hardware has become available which reduces the time required to process cross-correlation data to almost real-time. Hence, the only remaining obstacle in cross-correlation is the spatial resolution limitation which is easily solved by particle tracking. Here we have shown that the velocity vector map obtained via cross-correlation can be used as a guide for a fuzzy inference particle tracking operation leading to superior spatial resolution velocity estimates. The new technique has also been shown to perform well in the presence of large velocity gradients. The high data density obtained from the particle tracking is enhanced by color coding the velocity vector magnitudes, yielding a pseudo velocity contour map. The combined technique minimizes the sensitivity of PIV measurements to seed particle concentration. For high seed particle concentrations, cross-correlations are performed on small subregions and the particle tracking step improves the spatial resolution of the measured velocity vectors. For moderate to low seed particle cases the correlation subregion sizes are increased so that enough particles are present within the subregion to yield a good correlation. The particle tracking step is again applied to increase the spatial resolution of the measurements to be better than could be obtained alone via cross-correlation while still maintaining independence of the measurements.

The two-step procedure is not limited to cross-correlation. Auto-correlation may also be used on double exposure single image frame data. The fuzzy inference peak validation technique can again be used for maximized information recovery. The fuzzy inference particle tracking can also be applied in a second step for improved spatial resolution velocity measurements.

## REFERENCES

- Adamson, T.C. and Nicholls, J.A., 1959 "On the Structure of Jets From Highly Underexpanded Nozzles Into Still Air", *Journal of Aerospace Sciences*, pp 16-24, January.
- Funes-Gallanzi, M. and Bryanston-Cross, P.J., 1993 "Solid State Visualization of a Highly three Dimensional Flow Using Stereoscopic Particle Image Velocimetry (3DPIV)", *SPIE Conference on Optical Diagnostics in Fluid and Thermal Flow*, Vol 2005, San Diego, CA, pp 360-369, July 14-16.
- Host-Madsen, A. and McCluskey, D. R., 1994 "On the Accuracy and Reliability of PIV Measurements", *Seventh International Symposium on Applications of Laser Techniques to Fluid Mechanics*, pp 26.4.1-26.4.11, Lisbon, Portugal, July 11-14.
- Keane, R.D., Adrian, R.J., 1993 "Prospects for Super-Resolution with Particle Image Velocimetry", *SPIE Conference on Optical Diagnostics in Fluid and Thermal Flow*, Vol 2005, San Diego, CA, pp 283-293, July 14-16.
- Kemmerich, T and Rath, H. J., 1994 "Multi-Level Convolution Filtering Technique for Digital Laser-Speckle-Velocimetry", *Exper. in Fluids*, 17, pp 315-322.
- Krothapalli, A., Wishart, D. P., Lourenco, L. M., 1994 "Near Field Structure of a Supersonic Jet: 'On-Line' PIV Study" *Seventh International Symposium on Applications of Laser Techniques to Fluid Mechanics*, pp 26.5.1-26.5.6, Lisbon, Portugal, July 11-14.
- Meinhart, C.D., Prasad, A.K., Adrian, A.J., 1992 "Parallel Digital Processor System for Particle Image Velocimetry", *Sixth International Symposium on Applications of Laser Techniques to Fluid Mechanics*, pp 30.1.1-30.1.6, Lisbon, Portugal, July 11-14.
- Raffel, M., Leidl, B., Kompenhans, J., 1992 "Data Validation for Particle Image Velocimetry", *Sixth International Symposium on Applications of Laser Techniques to Fluid Mechanics*, pp 26.5.1-26.5.6, Lisbon, Portugal, July 11-14.
- Wernet, M. P., 1991 "Particle Displacement Tracking Applied to Air Flows", *Fourth International Conference on Laser Anemometry*, Cleveland, OH, pp 327-335, August 5-9.
- Wernet, M. P. and Pline, A., 1991 "Particle Image Velocimetry for the Surface Tension Driven Convection Experiment Using a Particle Displacement Tracking Technique", *Fourth International Conference on Laser Anemometry*, Cleveland, OH, pp 315-325, August 5-9.
- Wernet, M. P., 1993 "Fuzzy Logic Particle-Tracking Velocimetry", *SPIE Conference on Optical Diagnostics in Fluid and Thermal Flow*, Vol 2005, San Diego, CA, pp 701-708, July 14-16.

Westerweel, J. and Nieuwstadt, F.T.M., 1990 "Measurement of Dynamics of Coherent Flow Structures Using Particle Image Velocimetry" *Fifth International Symposium on Applications of Laser Techniques to Fluid Mechanics*, pp 18.3, Lisbon, Portugal, July 9-12.

Westerweel, J., Draad, A.A., van der Hoeven, J.G., van Oord, J., 1994 "A Fast Data Acquisition System for Digital PIV", *Seventh International Symposium on Applications of Laser Techniques to Fluid Mechanics*, pp 35.1.1-35.1.8, Lisbon, Portugal, July 11-14.

Willert, C.E. and Gharib, M., 1991, "Digital Particle Image Velocimetry", *Exper. in Fluids*, **10**, pp 181-193.



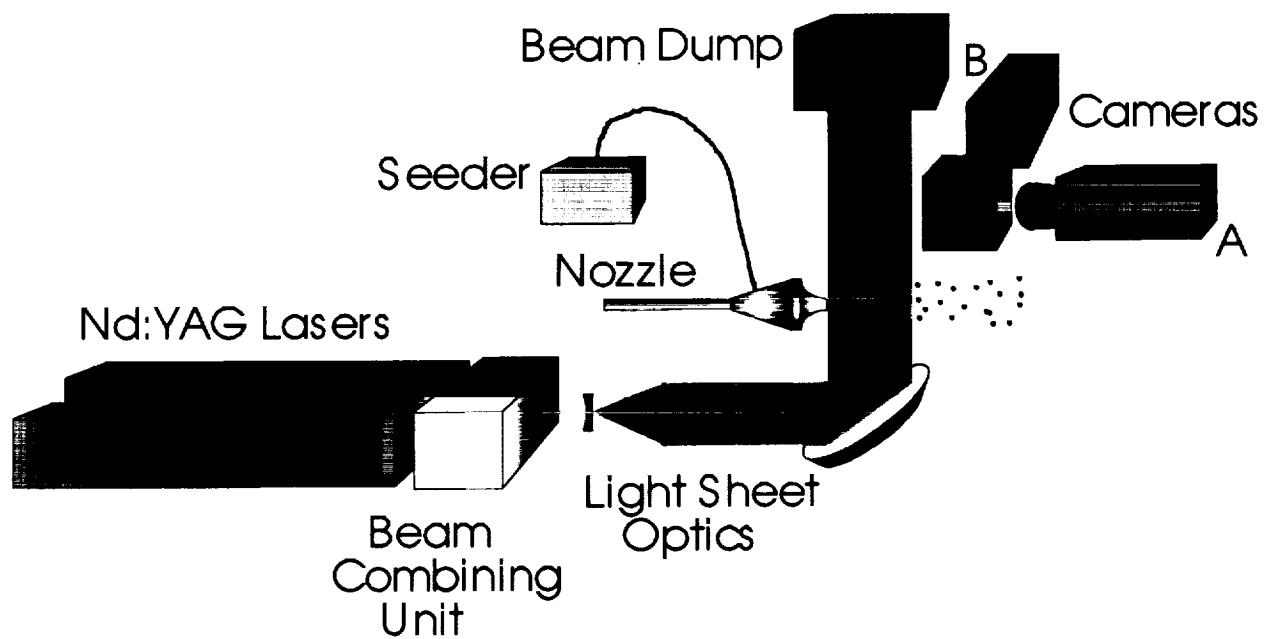


Figure 1.—Schematic drawing of optical system layout.



Figure 2.—Raw PIV image from camera. The location of the Mach disk is indicated by the vertical white line.

DOI: 10.1002/for

1000 1000 1000

[illegible]

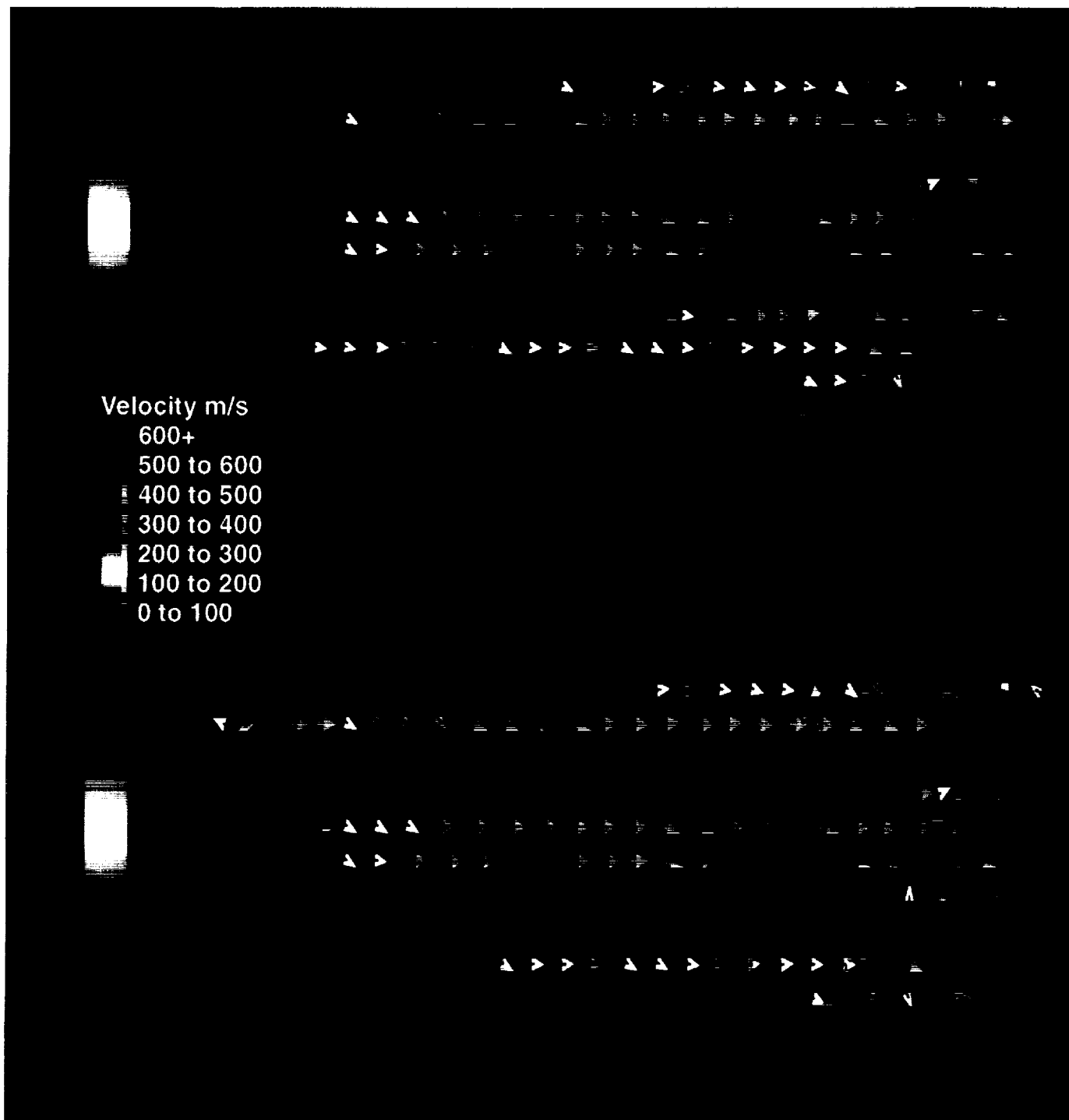


Figure 3.—(a) Cross-correlation vector map on 32x32 subregions with Fuzzy Inference correlation peak detection. The color bar indicates the velocity magnitude. (b) Cross-correlation vector map without peak detection step. Note the large number of spurious vectors on the periphery of the image.



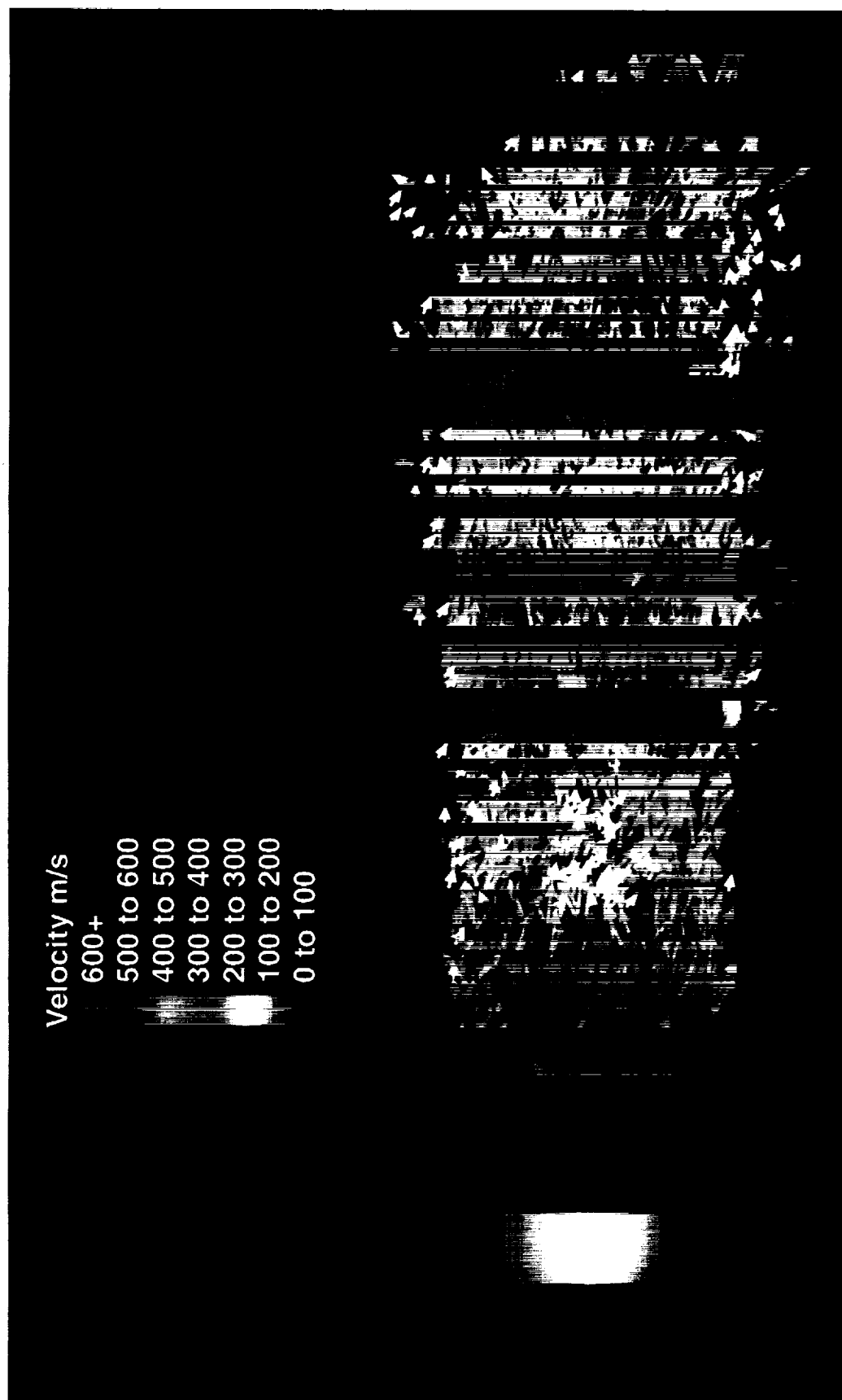


Figure 4.—Fuzzy Inference Particle Tracking velocity vector map. The high density of detected vectors results in higher spatial resolution measurements than the cross-correlation results.

1. The first part of the document is a list of the names of the members of the committee who have been appointed to study the problem of the

2. The second part of the document is a list of the names of the members of the committee who have been appointed to study the problem of the

3. The third part of the document is a list of the names of the members of the committee who have been appointed to study the problem of the

4. The fourth part of the document is a list of the names of the members of the committee who have been appointed to study the problem of the

5. The fifth part of the document is a list of the names of the members of the committee who have been appointed to study the problem of the

6. The sixth part of the document is a list of the names of the members of the committee who have been appointed to study the problem of the

7. The seventh part of the document is a list of the names of the members of the committee who have been appointed to study the problem of the

8. The eighth part of the document is a list of the names of the members of the committee who have been appointed to study the problem of the

9. The ninth part of the document is a list of the names of the members of the committee who have been appointed to study the problem of the

10. The tenth part of the document is a list of the names of the members of the committee who have been appointed to study the problem of the

11. The eleventh part of the document is a list of the names of the members of the committee who have been appointed to study the problem of the

12. The twelfth part of the document is a list of the names of the members of the committee who have been appointed to study the problem of the

13. The thirteenth part of the document is a list of the names of the members of the committee who have been appointed to study the problem of the

14. The fourteenth part of the document is a list of the names of the members of the committee who have been appointed to study the problem of the

15. The fifteenth part of the document is a list of the names of the members of the committee who have been appointed to study the problem of the

16. The sixteenth part of the document is a list of the names of the members of the committee who have been appointed to study the problem of the

17. The seventeenth part of the document is a list of the names of the members of the committee who have been appointed to study the problem of the

18. The eighteenth part of the document is a list of the names of the members of the committee who have been appointed to study the problem of the

19. The nineteenth part of the document is a list of the names of the members of the committee who have been appointed to study the problem of the

20. The twentieth part of the document is a list of the names of the members of the committee who have been appointed to study the problem of the

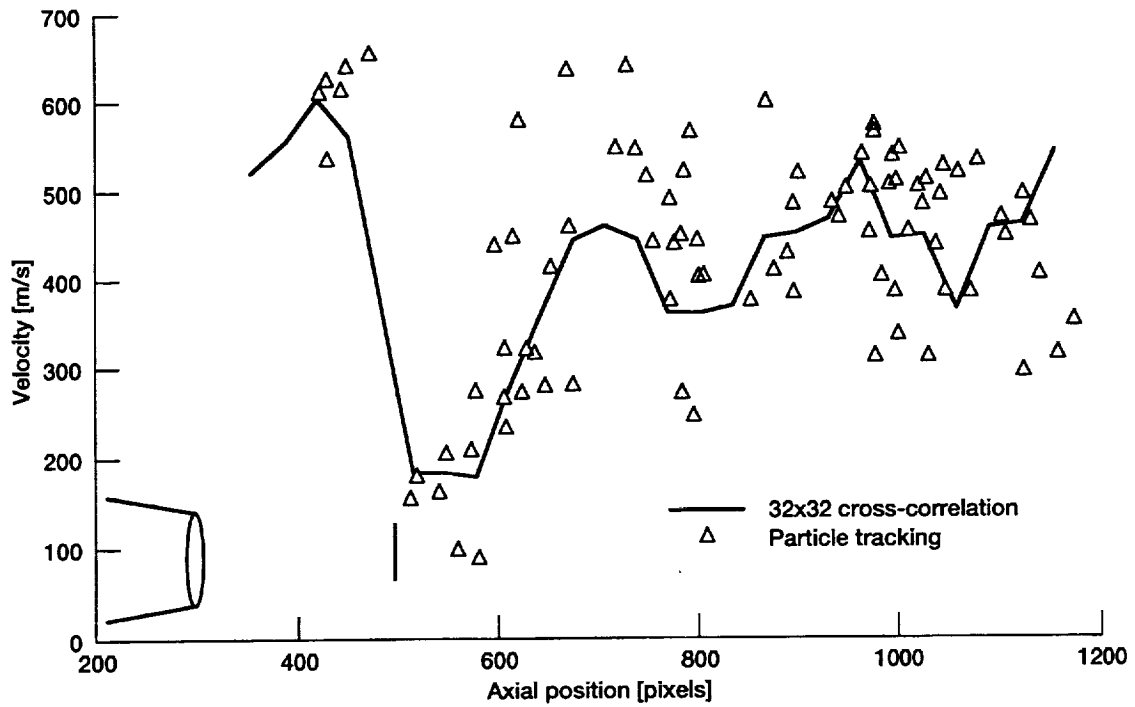


Figure 5.—Comparison of the nozzle centerline velocity for the correlation and particle tracking results. The correlation result is a smoother, low pass version of the individual particle tracking measurements.

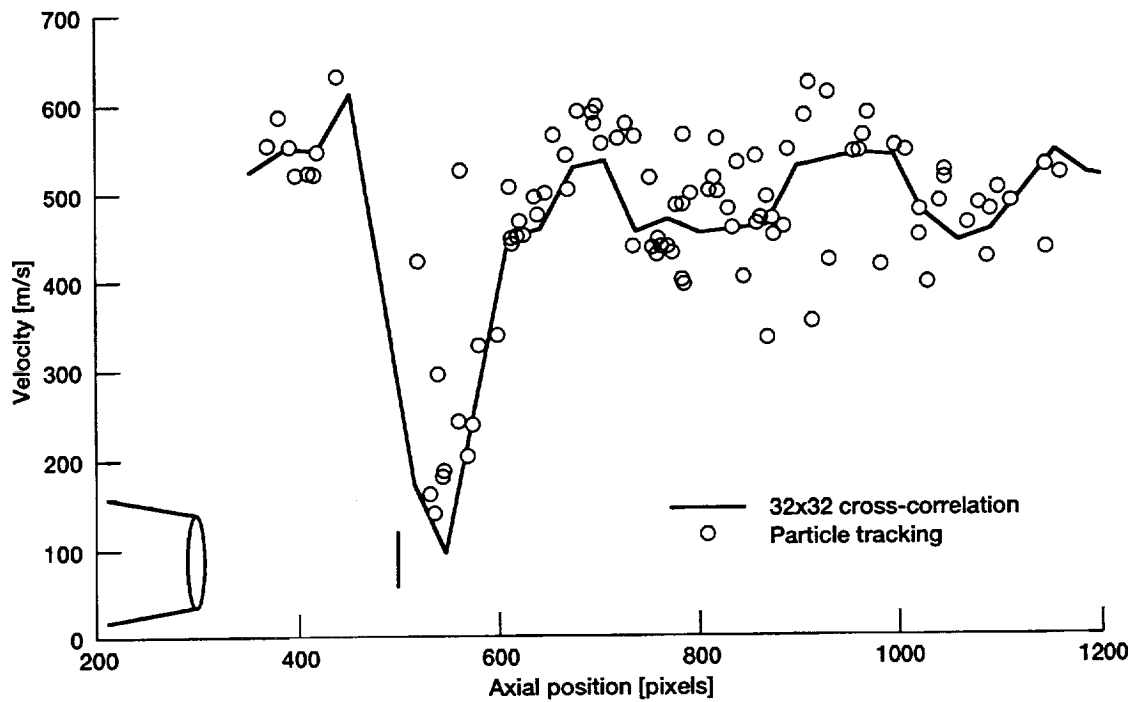


Figure 6.—Another comparison of the nozzle centerline velocity for the correlation and particle tracking results. The particle tracking result is more tightly grouped in this data set.

REPORT DOCUMENTATION PAGE			Form Approved OMB No. 0704-0188	
Public reporting burden for this collection of information is estimated to average 1 hour per response, including the time for reviewing instructions, searching existing data sources, gathering and maintaining the data needed, and completing and reviewing the collection of information. Send comments regarding this burden estimate or any other aspect of this collection of information, including suggestions for reducing this burden, to Washington Headquarters Services, Directorate for Information Operations and Reports, 1215 Jefferson Davis Highway, Suite 1204, Arlington, VA 22202-4302, and to the Office of Management and Budget, Paperwork Reduction Project (0704-0188), Washington, DC 20503.				
1. AGENCY USE ONLY (Leave blank)		2. REPORT DATE May 1995		3. REPORT TYPE AND DATES COVERED Technical Memorandum
4. TITLE AND SUBTITLE Fuzzy Inference Enhanced Information Recovery From Digital PIV Using Cross-Correlation Combined with Particle Tracking			5. FUNDING NUMBERS  WU-505-62-50	
6. AUTHOR(S)  Mark P. Wernet				
7. PERFORMING ORGANIZATION NAME(S) AND ADDRESS(ES)  National Aeronautics and Space Administration Lewis Research Center Cleveland, Ohio 44135-3191			8. PERFORMING ORGANIZATION REPORT NUMBER  E-9544	
9. SPONSORING/MONITORING AGENCY NAME(S) AND ADDRESS(ES)  National Aeronautics and Space Administration Washington, D.C. 20546-0001			10. SPONSORING/MONITORING AGENCY REPORT NUMBER  NASA TM-106896	
11. SUPPLEMENTARY NOTES Prepared for the Conference on Optical Techniques in Fluid, Thermal and Combusting Flows sponsored by the Society for Photo-Optical Instrumentation Engineers, San Diego, California, July 9-14, 1995. Responsible person, Mark P. Wernet, organization code 2520, (216) 433-3752.				
12a. DISTRIBUTION/AVAILABILITY STATEMENT  Unclassified - Unlimited Subject Category 35  This publication is available from the NASA Center for Aerospace Information, (301) 621-0390.			12b. DISTRIBUTION CODE	
13. ABSTRACT (Maximum 200 words) Particle Image Velocimetry provides a means of measuring the instantaneous 2-component velocity field across a planar region of a seeded flowfield. In this work only two camera, single exposure images are considered where both cameras have the same view of the illumination plane. Two competing techniques which yield unambiguous velocity vector direction information have been widely used for reducing the single exposure, multiple image data: cross-correlation and particle tracking. Correlation techniques yield averaged velocity estimates over subregions of the flow, whereas particle tracking techniques give individual particle velocity estimates. The correlation technique requires identification of the correlation peak on the correlation plane corresponding to the average displacement of particles across the subregion. Noise on the images and particle dropout contribute to spurious peaks on the correlation plane, leading to misidentification of the true correlation peak. The subsequent velocity vector maps contain spurious vectors where the displacement peaks have been improperly identified. Typically these spurious vectors are replaced by a weighted average of the neighboring vectors, thereby decreasing the independence of the measurements. In this work fuzzy logic techniques are used to determine the true correlation displacement peak even when it is not the maximum peak on the correlation plane, hence maximizing the information recovery from the correlation operation, maintaining the number of independent measurements and minimizing the number of spurious velocity vectors. Correlation peaks are correctly identified in both high and low seed density cases. The correlation velocity vector map can then be used as a guide for the particle tracking operation. Again fuzzy logic techniques are used, this time to identify the correct particle image pairings between exposures to determine particle displacements, and thus velocity. The advantage of this technique is the improved spatial resolution which is available from the particle tracking operation. Particle tracking alone may not be possible in the high seed density images typically required for achieving good results from the correlation technique. This two staged approach offers a velocimetric technique capable of measuring particle velocities with high spatial resolution over a broad range of seeding densities.				
14. SUBJECT TERMS  Velocimetry			15. NUMBER OF PAGES 17	
			16. PRICE CODE A03	
17. SECURITY CLASSIFICATION OF REPORT Unclassified	18. SECURITY CLASSIFICATION OF THIS PAGE Unclassified	19. SECURITY CLASSIFICATION OF ABSTRACT Unclassified	20. LIMITATION OF ABSTRACT	